Ding *et al. Environmental Microbiome* (2025) 20:163
https://doi.org/10.1186/s40793-025-00821-3

Environmental Microbiome

RESEARCH Open Access

The microbial community metabolic regime adapts to hydraulic disturbance in river–lake systems with high–frequency regulation

Jiewei Ding[1], Wei Yang[1,2*], Xiaoxiao Li[3], Xinyu Liu[1], Jiayue Zhao[1], Tao Sun[1,2] and Haifei Liu[1]

Abstract

Background River–lake ecosystems are crucial for the rational allocation of water resources, but frequent water diversion can destabilize water quality due to hydraulic disturbance. Microbial communities can respond rapidly to such external perturbations and influence these systems through the effects on nutrient metabolism. Therefore, understanding how microbial communities respond to hydraulic shocks in aquatic systems and whether they can adapt to such disturbances is essential for maintaining the health of river–lake systems. We used 16S rRNA and metagenomic sequencing technologies to examine the metabolic regimes of microbial communities during water regulation and non-regulation periods in river–lake systems.

Results We found that hydraulic disturbance tended to drive the microbial community toward homogenized selection, thereby weakening its stability. Flow velocity (*V*) and the nitrate (NO_3^-–N) concentration significantly affected microbial community composition and abundance, with clear threshold effects. We established low ($V = 0.284$ m/s, NO_3^-–N = 0.031 mg/L) and high ($V = 0.461$ m/s, NO_3^-–N = 0.055 mg/L) thresholds. These thresholds categorize microbial communities into three distinct regimes: regime1 (R1), regime 2 (R2), and regime 3 (R3). The microbial abundances in R1 and R3 were significantly higher than those in R2 ($p < 0.01$), while the community in R3 exhibited a strong denitrification capacity. In R3, the microbial community enhanced its denitrification metabolism by promoting the growth of denitrifying microbial genera (e.g., *Pseudomonas* and *Flavobacterium*) to counterbalance the impact of high *V* and NO_3^-–N. These strains contributed the denitrification-related genes *nasA*, *narB*, *nirB*, and *nirD* to the community, thereby promoting the NO_3^-–N metabolism and reducing environmental NO_3^-–N concentrations. In addition, we predicted microbial community abundance using an artificial neural network to validate the thresholds we identified.

Conclusions Our study provides theoretical support for understanding how microbial communities adapt to high-frequency hydraulic disturbances and offer valuable insights for managers to adjust water diversion strategies in a timely manner, thereby safeguarding the integrity of river–lake ecosystems.

Keywords River–lake ecosystems, Hydraulic disturbances, Microbial communities, Metabolic regimes, Threshold effects

*Correspondence:
Wei Yang
yangwei@bnu.edu.cn

Full list of author information is available at the end of the article

Graphical abstract

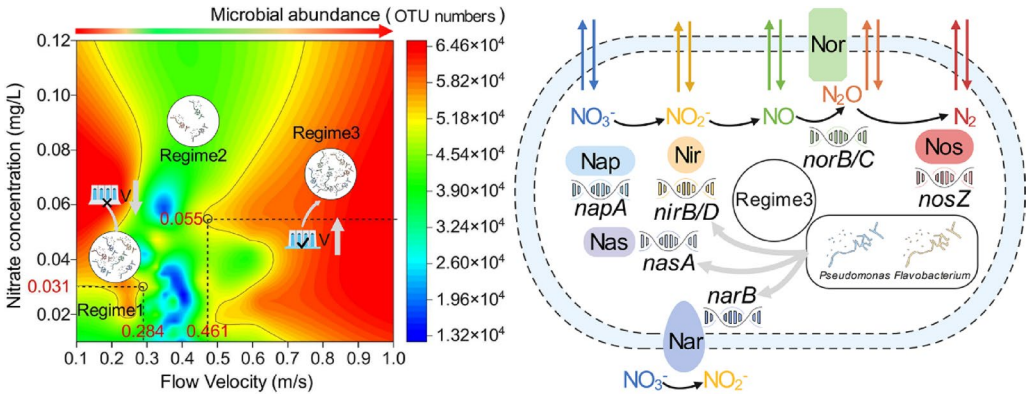

Background

The river–lake systems are integral hydrological units consisting of lakes and their interconnected rivers, processing the functions of material circulation, energy flow and ecological barrier [1, 2]. As globally distributed hydrological continuums [3, 4], river–lake systems are critical water conservation hubs that play a vital role in hydrological regulation while substantially contributing to socioeconomic development [5–7]. River–lake systems are important carriers of inter-basin water diversion systems used to alleviate the uneven distribution of water resources (such as the California State Water Project in USA, the West to East Water Transfer Project in Pakistan, the Colorado-Big Thompson Project and the South-to-North Water Diversion Project in China) [8, 9]. However, these frequent inter-basin water supply activities and the construction of water conservation facilities, such as gates and dams, have complicated the hydrodynamic conditions within these systems [10]. Hydraulic engineering management may induce significant hydraulic disturbance, potentially triggering sediment resuspension and consequent water quality deterioration [11]. These anthropogenic impacts on river–lake ecosystems have emerged as a critical environmental attention worldwide [12].

Water diversion will also affect a wide range of organisms within river–lake systems. Artificial regulation activities can fragment the habitats in these ecosystems, disrupt food chains, and threaten the survival of animals and plants [13, 14]. Moreover, the water quality degradation caused by regulation may trigger algal blooms, which can disrupt the ecological balance through impacts on phytoplankton and other communities [15, 16]. Furthermore, changes in the sediment deposition pattern during water diversion can lead to uneven nutrient distribution in the water. This poses a challenge for microbiomes that depend on specific nutrient ratios, as they must adapt to these altered conditions [17, 18]. It should be noted that among the many organisms affected by water diversion, microorganisms are sensitive and responsive to environmental changes. Changes in the composition and structure of bacterial communities therefore provide clues to the overall state of an ecosystem [19, 20]. This makes it necessary to clarify the impact of water regulation on microbial communities and determine whether they can adapt to the hydraulic disturbance caused by water regulation and can maintain the river–lake system's ecological health.

As fundamental components of river–lake ecosystems, microorganisms drive nutrient cycling, and this cycling is essential for maintaining the stability of the aquatic ecosystems [21–23]. Microorganisms can respond to perturbations in their environment and can adapt by adjusting their metabolic pathways [24–26]. Ren et al. [27] studied the river–lake system of China's Poyang Lake, and found that the deposition of organic matter and the input of exogenous nitrogen shaped microbial communities to promote organisms with strong metabolic potential for carbohydrates and nitrogen, both in the water and sediment. Similarly, Yuan et al. [28] found that microorganism in river channels were affected by concentrations of nitrite and dissolved oxygen. These environments can lead to proliferation of microorganisms that are efficient at denitrification and organic pollution degradation, thereby adapting to environmental disturbances caused by seasonal runoff. In addition, a recent study demonstrated that the sinking of algae in lakes can introduce sources of carbon, nitrogen, and phosphorus to surface sediments [29]. In response to this environmental change, the microbial community can adjust its metabolic potential, contributing more genes related to the conversion of nitrogen, phosphorus and carbon [30].

However, most previous studies focused on static water in river and lake systems. The lack of research on dynamic systems is an important gap in our knowledge, as there are complicated and dynamic hydrodynamic conditions

in river–lake systems, and particularly in those that are primarily used for inter-basin water transfer (such as China's South-to-North Water Diversion Project) [5]. On the one hand, the hydraulic shock created by flow management may induce the migration and succession of the original microbial community, which leads to instability of community composition and structure [31]. On the other hand, water diversion and hydraulic shocks may introduce additional pollution sources, such as nitrogen and phosphorus, that affect microbial community stability and alter the community's metabolic trends [18]. How microbial communities respond to these multiple forms of disturbance caused by complex hydrodynamic conditions, whether they can adapt to this environmental disturbance, and by what mechanism remain unclear.

Our study focuses on the Dongping river–lake system, an important water regulation lake for the Eastern Route of the South-to-North Water Diversion Project in China. The system receives inflows from the Dawen River (eastern side of the lake) [32] and the Liuchang River (southern side of the lake), and the lake sustains an aquaculture area near the outflow zone on its northern side. Therefore, its internal hydraulic conditions are complex. During regulation (R) periods, dynamic hydraulic changes will alter the original microbial community composition, potentially weakening community's stability [31]. In addition, internal pollution caused by hydraulic disturbances poses further challenges to microorganism survival [33]. Therefore, it is imperative to characterize the microbial community composition, its metabolic regime, and the driving mechanisms underlying community shifts during both R and non-regulation (NR) periods. In the present study of a Chinese river–lake system, our objectives were to (1) elucidate the community assembly patterns and stability of microbial communities during R and NR periods; (2) identify the key factors that affected the stability or changes of microbial communities; (3) explore the composition and metabolic patterns of microbial communities during the R and NR periods; and (4) reveal the key mechanisms by which microbial communities adapt to hydraulic disturbance. We hypothesized that the change between R and NR periods would drive changes in the water environment that would cause the microbial community to change in response. Our results provide insights into the identification and prediction of changes in microbial communities during different regulation periods, and will support the maintenance of stable river–lake ecosystems during high-frequency hydraulic shock periods.

Materials and methods

Study area and sampling area division

Our study area was the Dongping river–lake ecosystem. Dongping Lake is the last lake used to regulate water flows in the eastern route of China's South-to-North Water Diversion Project (SNWDP) (Fig. 1). It experiences an extended and high-frequency period of water transfer each year as water is channeled through diversion routes into the river–lake system [34]. The Dongping river–lake system has been conducting periodic water regulation every year since 2013 (China Ministry of Water Resources, CMWR) [35]. The most recent water regulation period, from September 23, 2022 to June 29, 2023. Water from the lower reaches of the Yangtze River flowed through the diversion channel into Dongping Lake, with a total regulation volume of 282 million cubic meters (Shandong Provincial Water Resources Department, SPWRD). We conducted sampling in April and

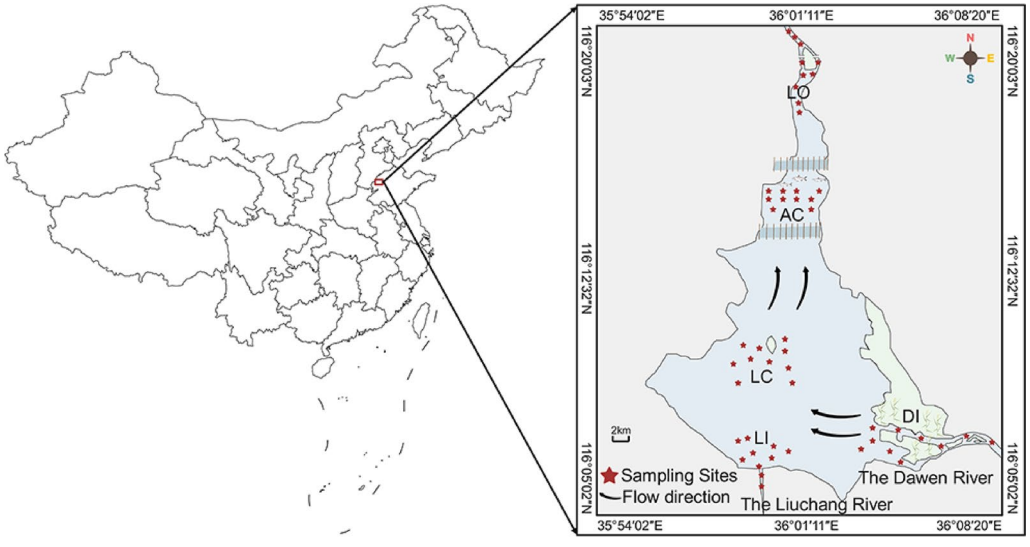

Fig. 1 Study area and locations of sampling points. AC, aquaculture zone; DI, Dawen River inflow zone; LC, lake center zone; LI, Liuchang River inflow zone; LO, lake outflow zone

August 2023 respectively, corresponding to the regulation and no-regulation periods.

We divided the study area into five distinct zones for sampling, based on the functions of different zones in the Dongping river–lake system and the design of the South-to-North Water Diversion Eastern Route. These zones were the Dawen River inflow zone (DI), the Liuchang River inflow zone (LI, which serves as the inflow channel from the SNWDP), the lake center zone (LC), an aquaculture zone (AC), and the lake's outflow zone (LO). Importantly, our zoning method also accounted for the flow field characteristics of the Dongping river–lake system (Fig. 1) [31]. This approach enhanced the scientific rigor and rationality of our sampling design.

Sampling and sequencing

According to the schedule of the SNWDP, the April was designated as the R period, and the August fell within the NR period [31]. In each zone, we established 10 sampling points to collect water samples. After three replicates, all subsamples were mixed into a composite sample. Water samples used for physicochemical property determination were stored at 4℃ and transported to the laboratory for testing within 6 h. For microbiological analysis, water samples were immediately pumped and filtered (see supplementary material for details), and the filter membranes were stored at -80℃ within 48 h [5]. Transparency (SD) was measured using Secchi disk. pH and dissolved oxygen (DO) were measured in situ using a HACH HQ30d portable measuring instrument (HACH, Loveland, CO, USA). Flow velocity (V) and water depth (D) were also determined on-site by using a Doppler current meter (SF-6526 J-21, Oriental Glass (Beijing) and a SpeedTech depth finder (SM-5A, Beijing, China), respectively. For water chemistry, total phosphorus (TP) was analyzed by the ammonium molybdate spectrophotometric method; phosphate (PO_4^{3-}), nitrate nitrogen (NO_3^-–N), and nitrite nitrogen (NO_2^-–N) by ion chromatography; total nitrogen (TN) through the alkaline potassium persulfate digestion-UV spectrophotometric method; ammonia nitrogen (NH_4^+–N) by Nessler's reagent spectrophotometry; total organic carbon (TOC) by the combustion oxidation-nondispersive infrared absorption method; and chemical oxygen demand (COD) by the dichromate method. All water sample analyses adhered to the testing standards and specifications of the Ministry of Ecology and Environment of the People's Republic of China [5]. Details testing standards and detection limits are provided in Table S1. We integrated 16S rRNA sequencing and metagenomic sequencing technologies to identify the microbial community's species composition and abundances, and performed gene annotation of the microbial communities during different periods. For 16S rRNA sequencing, we first extract the microbial DNA from samples. Using the extracted DNA as templates, we used primers 515F (5'-GTGCCAGC-MGCCGCGGTAA-3') and 806R (5'-GGACTACH-VGGGTWTCTAAT-3') to perform PCR amplification on the V3-V4 variable region of the 16S rRNA gene and constructed a sequencing library. Then we conduct sequencing data analysis. For metagenomic sequencing, we first extract the sample DNA, then construct the paired-end library, and then sequence and analyze the data. Details are provided in the supplementary material.

Statistical analyses

β nearest-taxon index (*βNTI*) based on a null model was used to assess the relative importance of deterministic and stochastic processes in microbiome assembly. According to the *βNTI* index, microbial assembly mechanisms were categorized into homogeneous selection (HoS), heterogeneous selection (HeS), homogenizing dispersal (HD), dispersal limitation (DL), and drift (DR) [36, 37]. Detailed calculation and classification criteria of *βNTI* are provided in the Supplementary material. The analysis was performed on the Majorbio cloud platform (https://cloud.majorbio.com/), a professional service platform in the microbiomics field specializing in high-throughput sequencing, multi-omics integration, and bioinformatics analysis technologies [38]. See supplementary material for a specific description. We calculated the average variation degree (*AVD*) to evaluate microbial community stability [39]. See supplementary material for specific calculations. Mantel test and Pearson correlation analysis were utilized on the Majorbio cloud platform to identify the driving factors that exhibited a significant association with the *AVD* [31]. To further explore the relationships between *AVD* and its influencing factors and assess the model goodness of fit [40, 41], we utilized the *mgcv* package for the R software to construct a generalized additive model and the *ggplot2* package for visualization [42]. The threshold is the critical level of the intensity of environmental disturbances that trigger significant nonlinear and persistent state changes in a system [43]. For microbial community, it refers to the critical point of environmental factors at which the community exhibits distinctly different species composition and abundance [44]. Accordingly, we defined the points where microbial abundance undergoes significant changes as threshold points. We conducted segmented regression analysis using the *segmented* package in R software to identify these threshold points (See supplementary material, Fig. S4 for details) [45, 46]. Following threshold determination, we used the *rug* plot features in the Origin software and the fitting regression and contour plots to characterize the distribution of microbial abundance related to environmental factors, thereby defining the microbial regimes [47]. We used the

Kruskal–Wallis non-parametric test to statistically validate the robustness of these threshold delineations (Fig. S5) [48]. We constructed a microbial co-occurrence network using the molecular ecological network analyses pipeline (MENAP) platform (http://ieg4.rccc.ou.edu/mena) based on stochastic matrix theory [49]. Specifically, the correlation matrix among microbial species was treated as a random matrix. By analyzing the statistical properties of its eigenvalues, we distinguished between genuine ecological relationships and randomly generated correlations [50, 51]. Genera with the top 1% in terms of the degree were classified as keystone microorganisms [31]. We used the *neuralnet* package for R to build an artificial neural network (ANN) model, and validated our microbial abundance predictions using the trained ANN model [52]. $R^2 = 0.62$ indicated that the model fitting effect was good [53]. Additionally, we used *ggplot2* to generate contour line plots, then we determined the threshold points predicted by the ANN model via identifying local extremums [54, 55]. One-way analysis of variance (ANOVA) was used to test the significance of the differences among the datasets.

Results

Assembly patterns and stability of the microbial communities

The results showed that during the R period, the primary assembly mechanism of the microbial community was HoS (Fig. 2A). The relative importance of HoS was 0.56 ± 0.11 (mean ± SE) across all zones, which was 0.19 higher than the value observed during the NR period (0.37 ± 0.14) (Fig. 2C). The mean *βNTI* value during the R period was 2.92 ± 1.71 (Fig. 2B), which illustrates the main role of HoS during this period. During the NR period, DR was the predominant assembly mechanism, with a mean relative importance of 0.49 ± 0.14, which was 0.11 higher than that during the R period (0.39 ± 0.09). In addition, the *βNTI* values of all zones except the LI zone during the NR period fell between −2 and 2 (Fig. 2D), indicating that DR was the primary driver of community dynamics. It is noteworthy that even during the NR period, HoS remained the dominant community assembly mechanism in the LI zone, where water transfer into the lake occurred, with a relative importance of 0.64.

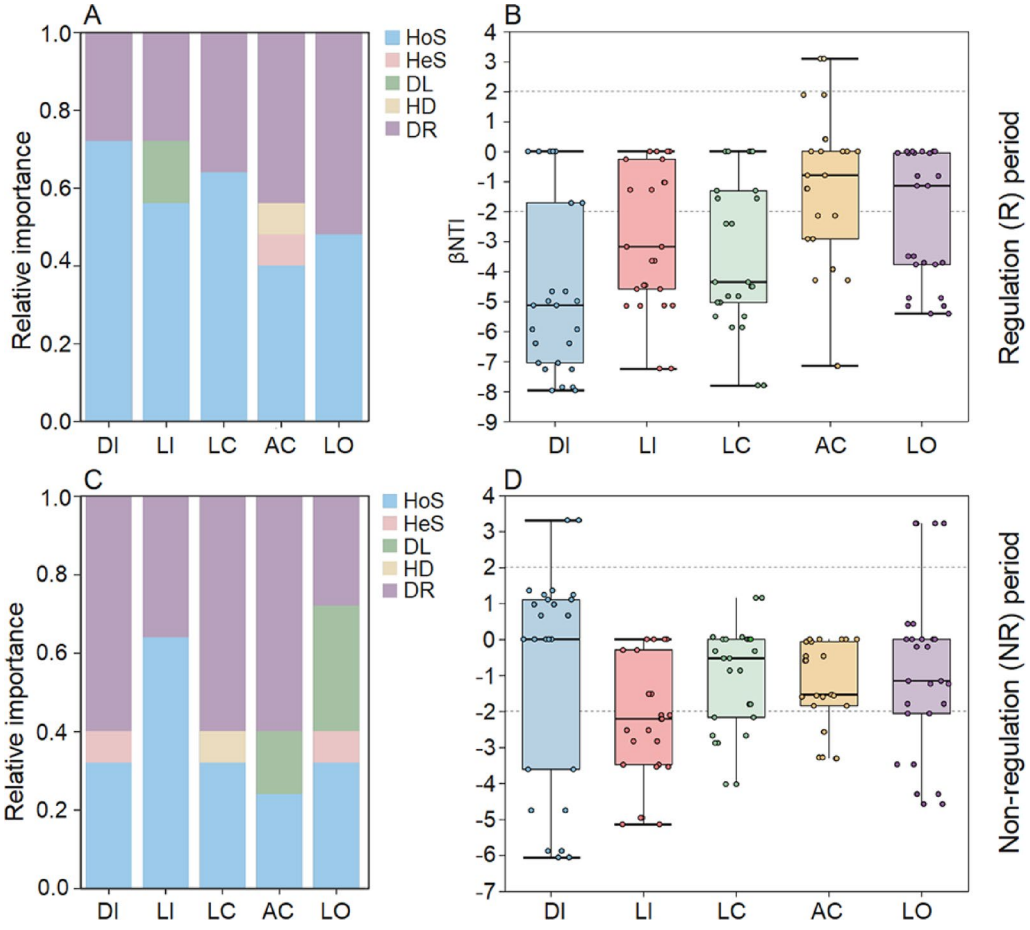

Fig. 2 Microbial community assembly patterns in the **A**, **B** R and **C**, **D** NR periods. Homogeneous selection (HoS), heterogeneous selection (HeS), homogenizing dispersal (HD), dispersal limitation (DL) and drift (DR)

The mean *AVD* index of the microbial community (Fig. 3A) was significantly higher during the R period (0.53 ± 0.03) than during the NR period (0.48 ± 0.02) ($p < 0.05$). Specifically, during the R period, no significant differences in AVD were found among zones ($p > 0.05$). However, the highest *AVD* values were observed in the LI zone (0.59 ± 0.06), which was 0.01, 0.09, 0.10 and 0.12 higher those in DI (0.58 ± 0.03), LO (0.50 ± 0.07), LC (0.49 ± 0.01), and AC (0.47 ± 0.02) zones, respectively. During the NR period, the LI zone (0.51 ± 0.06) remained the highest *AVD* value. Similarly, no significant differences were found among zones ($p > 0.05$), but the AVD value in the LI zone was 0.01, 0.03, 0.05 and 0.07 higher than those in AC (0.50 ± 0.02), DI (0.48 ± 0.05), LO (0.46 ± 0.04), and LC (0.44 ± 0.03) zones, respectively.

The key factors affecting the stability of microbial communities

We found that the trends of V (Fig. 3B) and NO_3^-–N (Fig. 3C) were consistent with the *AVD* values of the microbial community, while the other environment factors were not significantly correlated with *AVD* ($p > 0.05$) (Fig. S1). Therefore, determining key factors influencing microbial community *AVD* values was essential for our study. We ultimately identified NO_3^-–N, *V*, water depth (*D*), and pH as the key factors that influenced the *AVD* of the microbial community. During the R period (Fig. S2A), there was a significant positive correlation between NO_3^-–N and *AVD* ($r = 0.24$, $p < 0.05$), as was *V* ($r = 0.35$, $p < 0.01$). In the NR period (Fig. S2B), NO_3^-–N and *V* continued to show significant positive correlations with *AVD* ($r = 0.22$ and 0.27, respectively; both $p < 0.05$). And in the NR period, the correlation between pH and *AVD* showed a significant positive trend ($r = 0.28$, $p < 0.05$), but *D* was significantly negatively correlated with *AVD* ($r = 0.55$, $p < 0.01$) in the NR period. In addition, *V* and NO_3^-–N were strongly and significantly positively correlated during both the R period ($r = 0.73$, $p < 0.001$) and the NR period ($r = 0.79$, $p < 0.001$).

We further analyzed these variables using generalized additive models (Fig. 4). The results revealed weak but significant correlations between *V* and *AVD* ($R^2 = 0.29$, $p < 0.05$; Fig. 4A) and between NO_3^-–N and *AVD* ($R^2 = 0.21$, $p < 0.05$; Fig. 4C). In contrast, there were no significant correlations between *D* and *AVD* (Fig. 4B) or between pH and *AVD* ($p > 0.05$; Fig. 4D). However, the correlation between *V* and NO_3^-–N was significant and well-fitted ($R^2 = 0.66$, $p < 0.05$; Fig. 4E). Overall, *V* and NO_3^-–N most strongly influenced *AVD*, which suggests that *AVD* may be influenced by a combination of these variables rather than being controlled by a single variable.

Microbial community regimes and metabolic potential during different regulation periods

Our study revealed a distinct bimodal distribution of microbial abundance in response to changes in *V* (Fig. S3A) and NO_3^-–N (Fig. S3B). Specifically, microbial abundance was high at both low and high values of *V* and NO_3^-–N. Segmented regression analysis showed that the microbial community could be divided

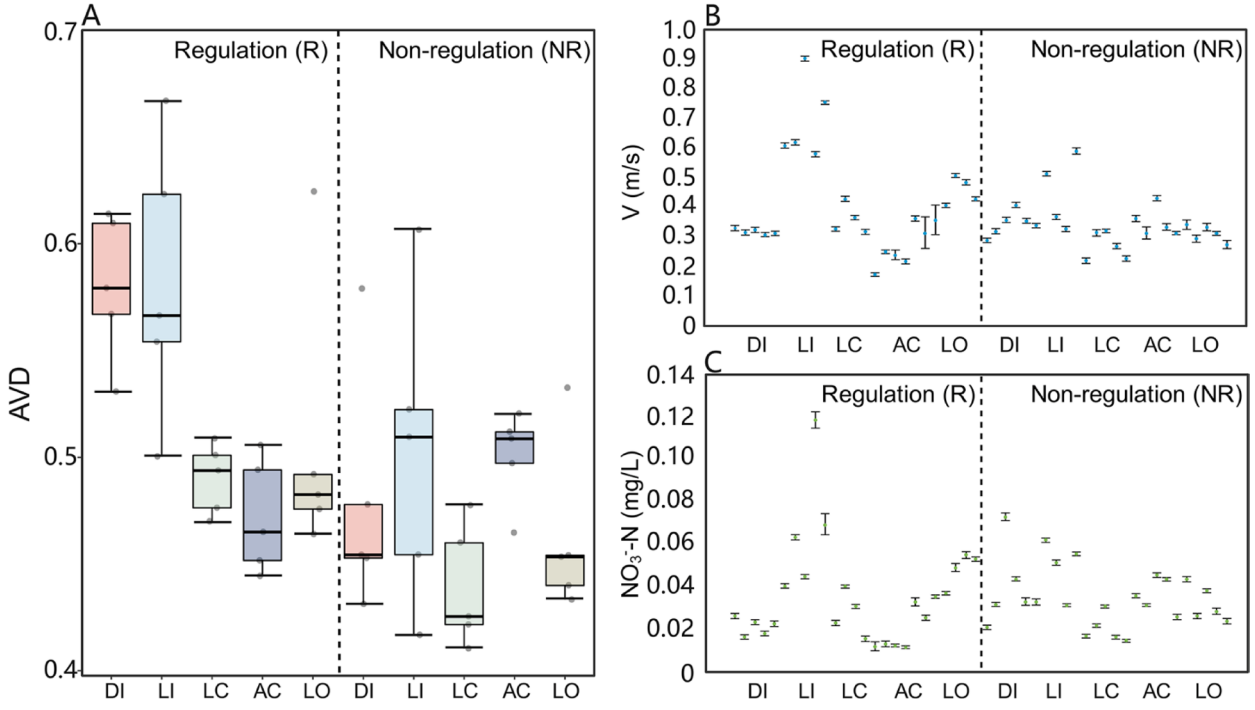

Fig. 3 **A** Average variation degree of microbial community and the changes in the **B** flow velocity and **C** nitrate concentration in the R and NR periods

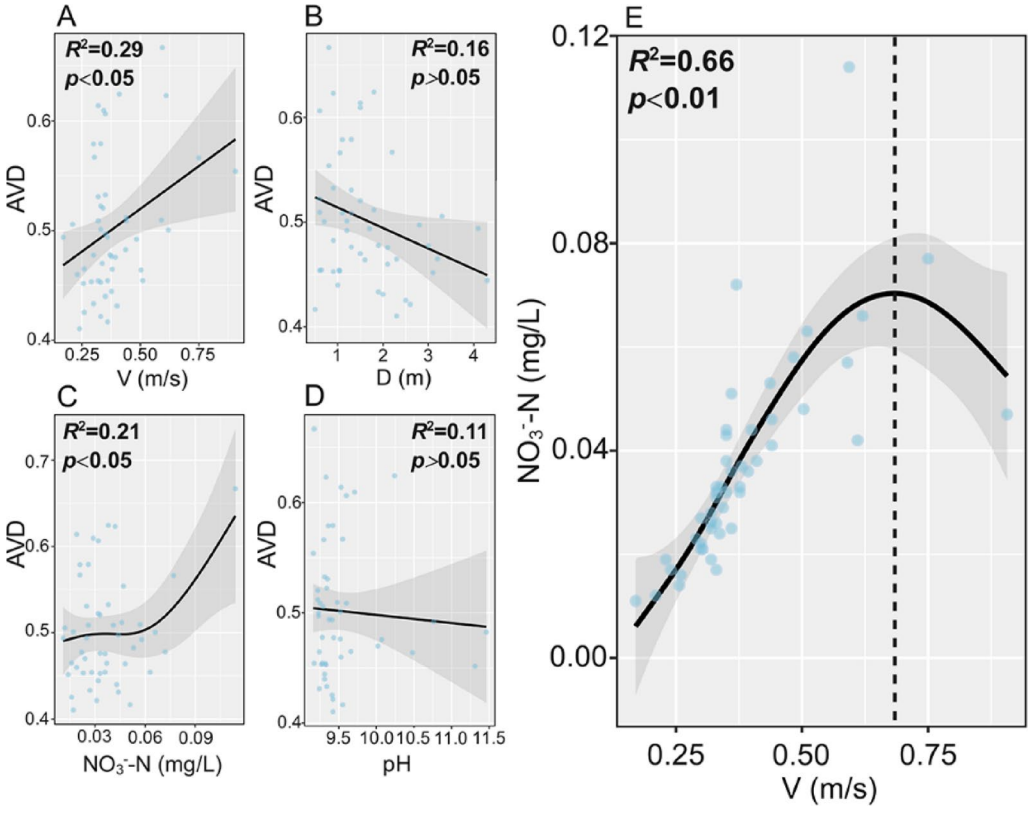

Fig. 4 Predicted relationships derived from generalized additive models for the relationships between **A** flow velocity (*V*) and the average variation degree (*AVD*), **B** water depth (*D*) and *AVD*, **C** nitrate (NO_3^-–N) concentration and *AVD*, and **D** pH and *AVD*. **E** Relationship between *V* and the NO_3^-–N concentration

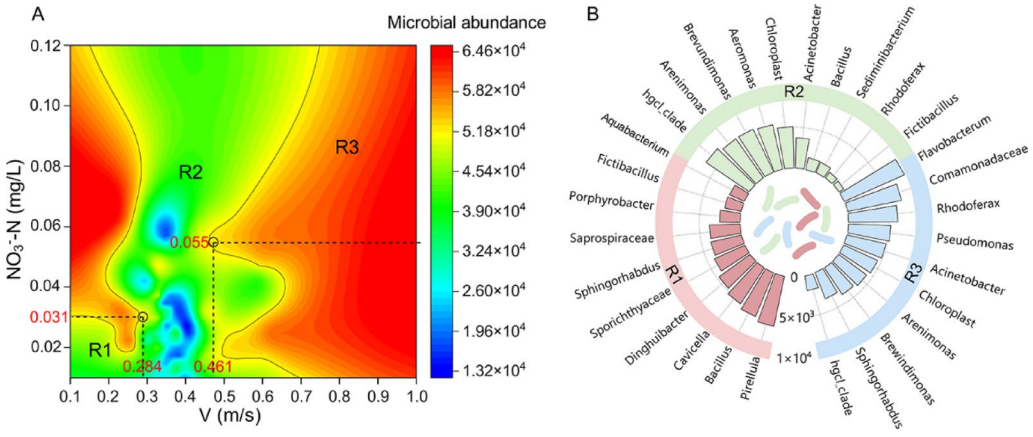

Fig. 5 Distribution of microbial community abundance under the different regimes: R1, below the low threshold, R2, between the two thresholds; and R3, above the high threshold. **A** Simultaneous effects of the two variables. **B** The community composition under the three regimes

into three intervals, with corresponding environmental thresholds identified (Fig. S4). The critical points of the regions with significant changes in abundance were shown in Fig. 5A. The impacts of *V* and NO_3^-–N on microbial abundance had significant threshold effects, with low (*V* = 0.284 m/s, NO_3^-–N = 0.031 mg/L) and high (*V* = 0.461 m/s, NO_3^-–N = 0.055 mg/L) thresholds. The microbial abundance was higher below the low threshold and above the high threshold, but decreased greatly between these two thresholds. We defined three microbial community regimes based on these thresholds: regime 1 (R1) below the low threshold, regime 2 (R2) between the two thresholds, and regime 3 (R3) above the high threshold, which were abundance aggregation intervals based on the microbial community abundance. The Kruskal–Wallis test revealed significant differences

Table 1 Characteristics of microbial co-occurrence networks

	Number of points	Number of links	Average degree	Average clustering coefficient	Modularity	Average path length
Regulation (R) period	171	276	4.700	4.43	0.70	4.43
Non-regulation (NR) period	160	326	3.223	5.46	0.72	5.46

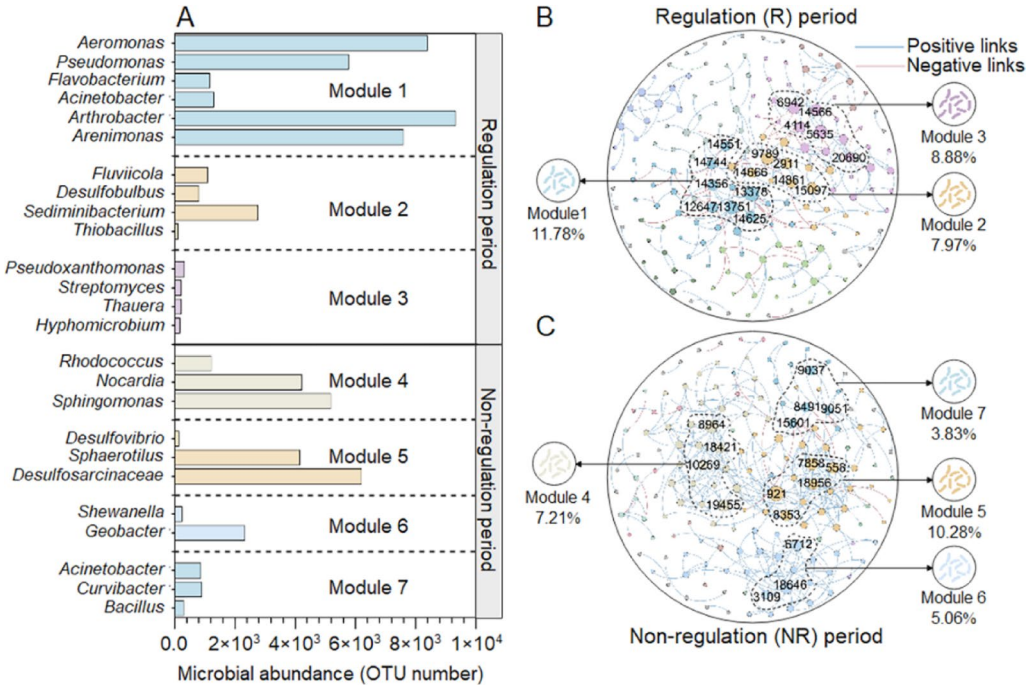

Fig. 6 **A** Composition of keystone taxa and **B** and **C** the proportions of connectivity within each module of the microbial co-occurrence networks during the R and NR periods, respectively. The number represents the microbial OUT serial number. Modules with similar functional potential are assigned the same color. OTU, operational taxonomic unit

in microbial abundance between R1 and R2 ($p < 0.001$), as well as between R2 and R3 ($p < 0.01$) (Fig. S5). However, no significant difference was observed between R1 and R3 ($p > 0.05$), which was consistent with our finding that microorganisms abundance showed a trend of increasing first and then decreasing with the elevation of V and NO_3^-–N concentration. These results confirmed the validity of our regime division. We found substantial differences in the composition of the microbial communities among these regimes (Fig. 5B). In R1, the microbial community was dominated by *Pirellula*, *Bacillus*, *Cavicella*, *Dinghuibacter*, and *Sporichthyaceae*. In R2, the dominant taxa were *hgcl_clade*, *Arenimonas*, *Brevundimonas*, *Aeromonas*, and *Chloroplast* was relatively abundant. In R3, the dominant microorganisms were *Flavobacterum*, *Comamonadaceae*, *Rhodoferax*, *Pseudomonas* and *Acinetobacter*. These results reveal clear differences in the composition of microbial communities across the three regimes. In particular, there was no significant difference ($p > 0.05$) in the abundance of the dominant microbial community in R3 and during the R period (Fig. S6).

We found that the microbial co-occurrence network showed different characteristics between R and NR periods (Table 1). Specifically, the microbial co-occurrence network during the NR period exhibited more links numbers (326) than in the R period (276). In addition, the number of points, the average degree, the average clustering coefficient (5.46), modularity (0.72), and average path length (5.46) were higher during the NR period. Furthermore, during the R period, the keystone microbial taxa were primarily clustered in three modules, which we designated as modules 1, 2, and 3 (Fig. 6B), in which a module refers to a group of microbial community subgroups with tight internal connections and sparse external connections, acting as the "functional units" of the network. These modules accounted for 11.8, 8.0, and 8.9% of the total microbial co-occurrence network, respectively. Module 1 included the keystone taxa *Aeromonas*, *Pseudomonas*, *Flavobacterium*, *Acinetobacter*, *Arthrobacter*, and *Arenimonas* (Fig. 6A). Module 2 was composed of *Fluviicola*, *Desulfobulbus*, *Sediminibacterium*, and *Thiobacillus*. Module 3 consisted of *Pseudoxanthomonas*, *Streptomyces*, *Thauera*, and *Hyphomicrobium*.

In contrast, during the NR period, the keystone microorganisms were mainly clustered into four modules, which we designated as Modules 4, 5, 6, and 7. The proportions of the keystone microbial degrees for these four modules in the whole network were 7.2, 10.3, 5.1, and 3.8%, respectively (Fig. 6C). The potential metabolic trends associated with the keystone taxa in each module are presented in Table S2.

The nitrogen metabolism pathways and related genes of the microbial community during the R and NR periods were shown in Fig. 7A. The abundance of denitrification-related genes was significantly higher during the R period ($p < 0.01$). This was particularly evident for the genes *narB*, *nasA*, *nirK*, *nirS*, *nirA*, *nirB*, and *nirD*, which exhibited notable abundances values of 1544, 3218, 8743, 6265, 12342 3546, and 3076 (OTUs), respectively. The numbers of other genes were shown in Table S3. Among them, *narB* is related to the coding for the NO_3^-–N assimilation system (Nas) enzyme and dissimilatory NO_3^-–N reductase (Nar) enzyme, and nasA is linked to the NO_3^-–N assimilation system (Fig. 7B). In addition, *nirA*, *nirB*, *nirD*, *nirK*, and *nirS* are all involved in the synthesis of nitrite reductase (Nir). These genes promote assimilatory NO_3^-–N reduction to ammonium, dissimilatory NO_3^-–N reduction to ammonium, anaerobic ammonium oxidation and denitrification metabolic processes, which reduced NO_3^-–N concentration. In addition, an interesting observation was that the relative abundances of the *amoA* (120), *amoB* (55), *amoC* (43), *hao* (22), *nxrA* (872), and *nxrB* (567) genes were significantly lower during the R period than those during the NR period ($p < 0.05$). Notably, all these genes were related to the nitrification process. Among these genes, *amoA*, *amoB*, and *amoC* are responsible for the synthesis of ammonia monooxygenase (Amo) enzyme, the *hao* gene is related to the synthesis of hydroxylamine oxidoreductase (Hao) enzyme, and *nxrA* and *nxrB* are involved in the synthesis of nitrite oxidoreductase (Nxr) enzyme (Fig. 7C). Under the action of these enzymes, the concentrations of ammonium and NO_2^-–N increased during the R period. Furthermore, we identified several microbial taxa, such as *Pseudomonas*, *Curvibacter*, *Acidovorax*, and *Flavobacterium*, these strains collectively contributed three or more genes related to denitrification metabolism (Fig. 7D). These taxa may play a crucial role in driving community-level nitrogen cycling during the R period.

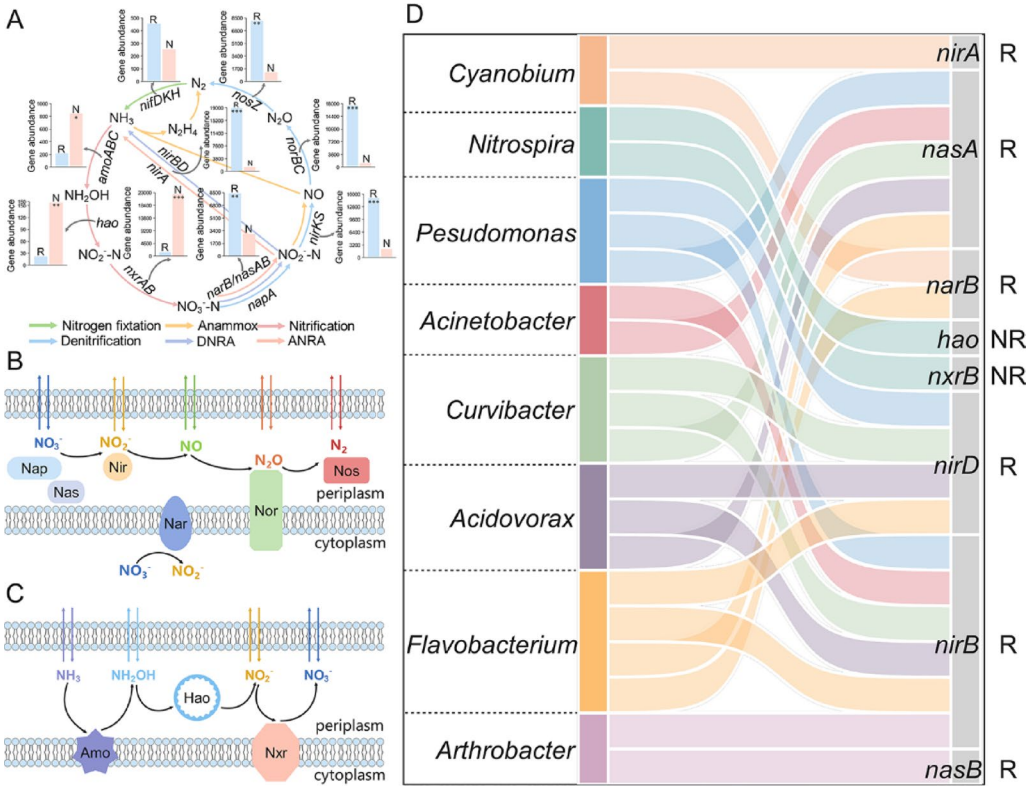

Fig. 7 **A** Nitrogen metabolism process of the microbial communities during the water R and NR periods. Anammox, anaerobic ammonium oxidation; ANRA, assimilatory nitrate (NO_3^-–N) reduction to ammonium; DNRA, dissimilatory NO_3^-–N reduction to ammonium. **B** important enzymes involved in nitrogen metabolism during the water regulation period: Nap, periplasmic nitrate reductase; Nar, nitrate reductase; Nas, assimilatory nitrate reductase; Nir, nitrite reductase; Nor, nitric-oxide reductase; and Nos, nitric-oxide synthase. **C** important enzymes involved in nitrogen metabolism during the water non-regulation period: Amo, ammonia monooxygenase; Hao, hydroxylamine oxidoreductase; and Nxr, nitrite oxidoreductase. **D** microorganisms that contributed genes related to nitrogen metabolism during the regulation (R) and non-regulation (NR) period

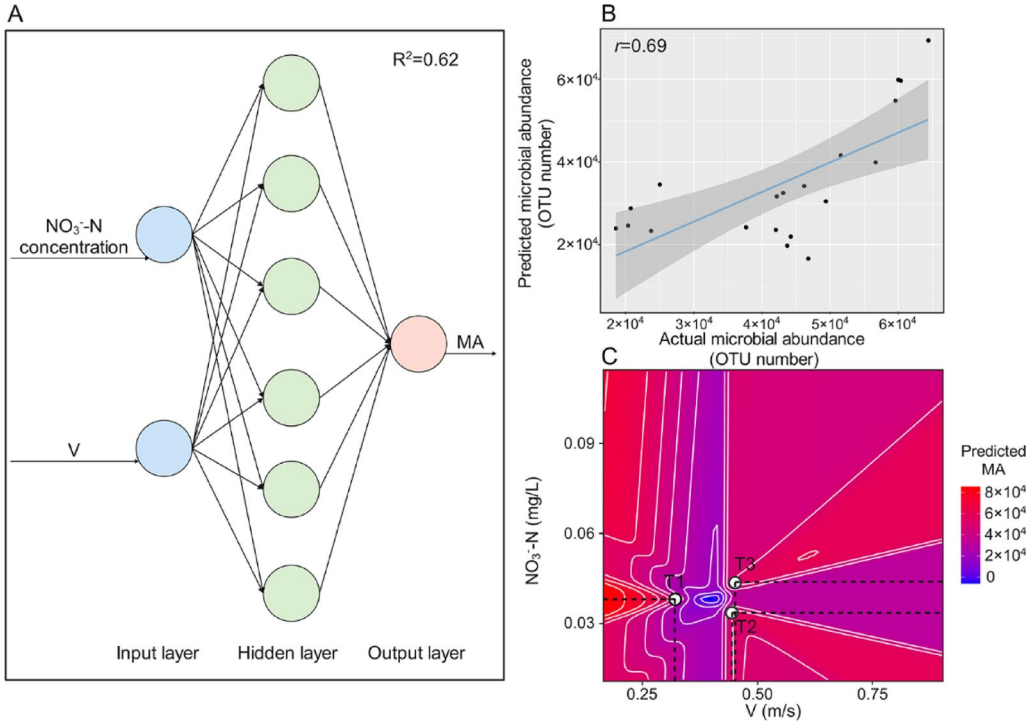

Fig. 8 **A** Structure of the artificial neural network model. **B** Prediction of the microbial abundance (*MA*) using an artificial neural network model. **C***MA* as a function of the nitrate (NO_3^-–N) concentration and flow velocity (*V*). T1 to T3 represent three potential thresholds

Table 2 Thresholds (T1 to T3) predicted by the artificial neural network model for flow velocity (*V*) and nitrate (NO_3^-–N) concentration

Threshold point	*V* (m/s)	NO_3^-–N (mg/L)
T1	0.325	0.038
T2	0.448	0.034
T3	0.453	0.043

Identification and prediction of microbial community status

We developed an ANN model to predict and evaluate the structure of the microbial community and abundance of various taxa. The input layer consisted of two key variables (*V* and the NO_3^-–N concentration), which we had previously identified as significantly influencing microbial abundance. The input layer comprised two neurons, the hidden layer comprised six neurons, and the output layer represented microbial community abundance (Fig. 8A). The model's predictions showed a good correlation with the actual values of microbial abundance ($R^2 = 0.62$ Fig. 8A) ($r = 0.69$, $p < 0.05$; Fig. 8B). In addition, we used the trained model to simulate microbial abundance values under various *V* and NO_3^-–N conditions to identify potential critical threshold points. We detected three possible thresholds (Fig. 8C), which we labeled as T1 ($V = 0.325$ m/s, NO_3^-–N = 0.038 mg/L), T2 ($V = 0.448$ m/s, NO_3^-–N = 0.034 mg/L), and T3 ($V = 0.453$ m/s, NO_3^-–N = 0.043 mg/L) (Table 2).

Discussion

Flow velocity significantly affected the microbial community composition

Our research revealed that hydraulic disturbances led to a shift in the microbial community assembly mechanisms towards homogeneous selection, thereby making the community composition more similar. High *V* reduced the stability of the microbial community. During the water regulation period, a substantial influx of water from the SNWDP increased flow velocity, thereby creating hydraulic disturbance and altering the existing water levels [56]. This short-term increase in *V* led to sediment resuspension, which in turn cause elevated nitrogen concentrations in the water [31]. This resulting high nitrogen loads created a homogenous selection environment for microorganisms, and potentially promoted species adaptation or elimination within the microbial community [57]. This process led to a more similar microbial community composition in areas affected by the hydraulic disturbance.

Even during the non-regulation period, microbial communities in the Liuchang River inflow zone were still dominated by homogeneous selection processes, which confirmed the influence of high *V* on community composition. In addition, we found that during the non-regulation period, the microbial community assembly in most zones was mainly driven by drift; that is, cell division, replication, lysis, mortality, growth, and survival of

microbial individuals affected the community composition [58]. This may be due to the relatively stable water flow during this period, which would have exerted lower environmental selection pressure on the microbial community. As a result, species would exhibit similar competitiveness for resource acquisition [59]. Therefore, the species turnover and community composition changes were largely dominated by the stochastic processes related to drift.

During the regulation period, the microbial communities had high *AVD* values, but this means that community stability was low [60]. In addition, the microbial communities exhibited shorter average path lengths and high average degrees under high *V*, which suggested closer interactions among species and a rapid response to external disturbance [61]. However, this also indicated that community composition was highly dynamic, and that the original structure was unable to persist in the face of intense hydraulic disturbances, resulting in weak community stability [62]. In addition, during the regulation period, high *V* increased nitrogen loads in the water body, shortened the contact time between microorganisms and pollutants, and affected the discharge of microbial metabolites [63]. These changes likely favored the persistence of genera that can tolerate or benefit from high NO_3^-–N concentrations while eliminating those with low tolerance. Furthermore, the microbial community might change to increase the number of new genera that could adapt to or take advantage of elevated nitrogen loads [64], leading to significant shifts in community composition and reduced community stability. Therefore, the effect of *V* on microbial community composition is substantial and should not be overlooked.

Microorganisms adapt to hydraulic pulses through changes in the metabolic balance

We found that microbial communities can adapt to water disturbance by balancing their metabolic processes, with *V* and the NO_3^-–N concentration emerging as key factors that influenced the entire process. During the regulation period, hydraulic shocks increased *V*, which may cause the sediment to be suspended again, thereby increasing the NO_3^-–N concentration [5]. Confronted with high *V* and NO_3_N levels, microbial communities may exhibit changes in their metabolic process to enhance nitrogen resource utilization efficiency [65–67]. This adjustment lets them achieve metabolic process balance, improve survival and growth, and better adapt to the new environmental conditions. It's worth emphasizing that, compared to the non-regulation period that is characterized by low *V*, microbial communities during the regulation period exhibited distinct metabolic patterns, with significant changes in community composition and function.

In addition, the dominant and keystone species showed stronger nitrogen metabolic potential, especially with the appearance of genera capable of denitrification. The microbial community also showed high expression of genes related to denitrification processes. During the regulation period, several dominant microorganisms in the community, including *Flavobacterium* [68], *Rhodoferax* [69], *Comamonadaceae* [70], *Arenimonas* [71], *Pseudomonas* [72], and *Thiobacillus* [73] have been confirmed to exhibit an ability to remove nitrogen. Importantly, *Arenimonas*, *Pseudomonas*, and *Flavobacterium* also served as keystone microorganisms during this period. In addition, *Pseudomonas* and *Flavobacterium* were important contributors of genes related to nitrogen metabolism, as they provided *narB*, *nirB*, *nirD*, and *nasA*, which are associated with denitrification. This agrees with similar previous studies [68, 74, 75]. These genes are involved in the synthesis of Nar, Nir and Nas enzymes that promote NO_3^-–N metabolism [76, 77]. Therefore, NO_3^-–N was transformed to NO_2^-–N under the catalysis of Nar and Nas enzymes, then converted to NO and N_2O by Nir enzymes, and finally converted to N_2. Meanwhile, the expression levels of genes such as *hao*, *nxrA*, and *nxrB* decreased. This inhibited the synthesis of Amo, Hao, and Nxr enzymes by these genes, so restricting the nitrification process, and reducing the utilization of ammonium and nitrites [78]. These metabolic processes enable microorganisms to metabolize excess NO_3^-–N and adapt to the hydraulic disturbance caused by water regulation.

Our results also revealed that *V* and the NO_3^-–N concentration exerted significant threshold effects on the microbial community abundance. Specifically, lower and higher *V* thresholds corresponded to two distinct NO_3^-–N concentration thresholds. This suggests that at lower *V*, most microorganisms can adapt and maintain normal function, resulting in no clear metabolic preference by the community for any particular substance. For instance, at low *V*, the community comprises a diverse array of microorganisms involved in a range of metabolic processes: Module 4 is associated with carbon metabolism, Module 5 with sulfur metabolism, Module 6 with iron reduction, and Module 7 with nitrogen and phosphorus conversion. However, once *V* exceeded the higher threshold, those microorganisms that could not adapt quickly to the high *V* and nitrogen load would be eliminated, leaving only highly resilient genera to survive [64].

Consistent with this, we found that as the *V* and NO_3^-–N concentration increased, the abundance of microorganisms decreased significantly between the low and high threshold intervals (i.e., in R2). When flow *V* and the NO_3^-–N concentration reached the higher threshold, the competitive dynamics among microorganisms shifted to favor the proliferation of dominant genera capable of resisting external stresses. For example,

at the higher threshold (R3), genera such as *Flavobacterium*, *Comamonadaceae*, *Pseudomonas*, and *Rhodoferax* emerged, driving an increase in the microbial community abundance. These highly resilient microorganisms drove the whole community's nitrogen cycling towards denitrification through adjustments of their metabolic patterns. This, in turn, decreased the external NO_3^-–N concentrations. This confirmed our finding that during the R period, microorganisms tend more to assimilatory nitrate reduction to ammonium, dissimilatory NO_3^-–N reduction to ammonium, anaerobic ammonium oxidation, and denitrification process. Conversely, the nitrification process was weakened, which lead to a certain degree increase in the concentrations of ammonium and NO_2^-–N, while the concentration of NO_3^-–N decreased. This also explains why the NO_3^-–N concentration in our study did not consistently increase with increasing *V*.

In addition, we developed an ANN model based on actual measurements and used it to predict community abundance under various combinations of *V* and NO_3^-–N concentration. The model confirmed the threshold effects of the two variables on microbial abundance, with predicted results closely aligning with measured results. This further enhances our understanding of the microbial community dynamics. Our findings provide valuable insights for river–lake system managers, as they will help them to tailor water diversion strategies to account for nutrient loads. This approach can maximize microbial community metabolism and stabilize the aquatic environment.

Conclusions

In our study, we examined the metabolic dynamics of microbial communities during different regulation periods in the Dongping river–lake system. We confirmed our hypothesis that the environmental change between regulation and non-regulation periods changed the water environment in ways that caused the microbial community to change in response. During these periods, high-frequency hydraulic disturbances caused increased NO_3^-–N concentrations. These external environmental perturbations drove microbial community assembly patterns toward homogenization, which decreased the stability of the community composition.

In addition, we found that the microbial community abundance was primarily influenced by *V* and the NO_3^-–N concentration, with distinct thresholds observed for their effects. Specifically, microbial abundance was higher in regions with low and high threshold values, but lower in regions between these thresholds. The variation in abundance was likely due to the emergence of genera such as *Pseudomonas* and *Flavobacterium*, which possess high nitrogen metabolic capacities. These genera proliferated in response to disturbances caused by high *V* and NO_3^-–N concentrations. Finally, we employed an artificial neural network to predict microbial abundance based on *V* and the NO_3^-–N concentration, thereby validating the identified thresholds. Our study provides novel insights into assessing the health of river–lake ecosystems through the lens of microbial metabolism. However, our study only compared the microbial metabolic differences between water regulation and non-regulation periods of river–lake systems, and lacks long-term dynamic monitoring data on the external environment. This limitation makes it difficult for our conclusions to reflect the impacts of long-term interannual hydrological and climatic changes on the microbial communities, thereby restricting the extrapolation of this study's finding to some extent. It will be necessary to carry out continuous observation and analysis in the future to obtain more generalizable inferences.

Supplementary Information

The online version contains supplementary material available at https://doi.org/10.1186/s40793-025-00821-3.

Supplementary Material 1

Acknowledgements
We are grateful to Majorbio Co., Ltd. (Shanghai, China) for assisting in the bioinformatics analysis of this manuscript.

Author contributions
Jiewei Ding: Writing—original draft, Data curation, Visualization, Investigation. Wei Yang: Writing—review & editing, Supervision, Funding acquisition. Xiaoxiao Li: Investigation, Methodology. Xinyu Liu: Investigation. Jiayue Zhao: Data curation. Tao Sun: Writing—review & editing, Resources. Haifei Liu: Methodology, Software.

Funding
This work was supported by the National Key Research and Development Program of China (No. 2023YFC3209003), and by the Major Scientific and Technological Innovation Projects in Shandong Province (2021CXGC011201).

Data availability
We have uploaded the 16 S rRNA gene amplicon sequences and metagenomic sequences to the NCBI Sequence Read Archive (SRA) with the accession number PRJNA1281048 (https://www.ncbi.nlm.nih.gov/bioproject/PRJNA1281048). And other data were all provided in this study.

Declarations

Competing Interests
The authors declare no competing interests.

Author details
[1]State Key Laboratory of Regional Environment and Sustainability, School of Environment, Beijing Normal University, No. 19 Xinjiekouwai St., Haidian District, Beijing 100875, China
[2]Yellow River Estuary Wetland Ecosystem Observation and Research Station, Ministry of Education, Dongying, China
[3]School of Biosciences, University of Sheffield, Sheffield S10 2TN, UK

Received: 31 May 2025 / Accepted: 5 November 2025
Published online: 25 November 2025

References

1. Potasznik A, Szymczyk S. Magnesium and calcium concentrations in the surface water and bottom deposits of a river-lake system. J Elem. 2015;20:677–92. https://doi.org/10.5601/jelem.2015.20.1.788.
2. Guo W, Yang H, Ma Y, Hong F, Wang H. Comprehensive evaluation of the hydrological health evolution and its driving forces in the river-lake system. Ecol Inform. 2023;75:102117. https://doi.org/10.1016/j.ecoinf.2023.102117.
3. Battin TJ, Lauerwald R, Bernhardt ES, Bertuzzo E, Gener LG, Hall R Jr, et al. River ecosystem metabolism and carbon biogeochemistry in a changing world. Nature. 2023;613:449–59. https://doi.org/10.1038/s41586-022-05500-8.
4. Jia J, Gao Y, Qin B, Dungait JAJ, Liu Y, Lu Y, et al. Evolving geographical gross primary productivity patterns in global lake systems and controlling mechanisms of associated phytoplankton communities since the 1950s. Earth-Sci Rev. 2022;234:104221. https://doi.org/10.1016/j.earscirev.2022.104221.
5. Ding J, Yang W, Liu X, Zhao Q, Dong W, Zhang C, et al. Unraveling the rate-limiting step in microorganisms' mediation of denitrification and phosphorus absorption/transport processes in a highly regulated river-lake system. Front Microbiol. 2023;14:1258659. https://doi.org/10.3389/fmicb.2023.1258659.
6. Wang S, Ran F, Li Z, Yang C, Xiao T, Liu Y, et al. Coupled effects of human activities and river-lake interactions evolution alter sources and fate of sedimentary organic carbon in a typical river-lake system. Water Res. 2024;255:121509. https://doi.org/10.1016/j.watres.2024.121509.
7. Wu S, Dong Y, Stoeck T, Wang S, Fan H, Wang Y, et al. Geographic characteristics and environmental variables determine the diversities and assembly of the algal communities in interconnected river-lake system. Water Res. 2023;233:119792. https://doi.org/10.1016/j.watres.2023.119792.
8. Shi Z, Huo S. Research status and prospect of water ecological and environmental impacts of inter-basin water diversion projects. Sci Technol Foresight. 2025;4:29–41. https://doi.org/10.3981/j.issn.2097-0781.2025.03.003.
9. Lu L, Chen Y, Li M, Lei X, Ni Q, Liu Z. Spatiotemporal characteristics and potential pollution factors of water quality in the eastern route of the South-to-North Water Diversion Project in China. J Hydrol. 2024;638:131523. https://doi.org/10.1016/j.jhydrol.2024.131523.
10. Yang X, Zhang S, Tang C, Wu C, Ge Y. Impact of Three Gorges Dam construction on spatiotemporal variations in the hydrodynamic regime of Poyang Lake (China). J Hydrol. 2025;646:132302. https://doi.org/10.1016/j.jhydrol.2024.132302.
11. Cofalla C, Hudjetz S, Roger S, Brinkmann M, Frings R, Woelz J, et al. A combined hydraulic and toxicological approach to assess re-suspended sediments during simulated flood events-part II: an interdisciplinary experimental methodology. J Soils Sediments. 2012;12:429–42. https://doi.org/10.1007/s11368-012-0476-2.
12. Scanlon BR, Fakhreddine S, Rateb A, de Graaf I, Famiglietti J, Gleeson T, et al. Global water resources and the role of groundwater in a resilient water future. Nat Rev Earth Environ. 2023;4:87–101. https://doi.org/10.1038/s43017-022-00378-6.
13. He F, Zarfl C, Tockner K, Olden JD, Campos Z, Muniz F, et al. Hydropower impacts on riverine biodiversity. Nat Rev Earth Environ. 2024;5:755–72. https://doi.org/10.1038/s43017-024-00596-0.
14. Lu X, Ren J, Gao D, Yin L, Dou J, Li H, et al. Impacts of hydrodynamic variation on submerged macrophytes in lakes: a review. Acta Ecol Sin. 2022;42:4245–54. https://doi.org/10.5846/stxb202012243261.
15. Chen L, Wan N, Liu B, Liu G, Zhang Y. Effect of water diversion on phytoplankton in the Jihongtan reservoir revealed by eDNA. Environ Sci Technol. 2024;47:80–8. https://doi.org/10.19672/j.cnki.1003-6504.1978.23.338.
16. Hou X, Hu X, Li Y, Zhang H, Niu L, Huang R, et al. From disruption to adaptation: response of phytoplankton communities in representative impounded lakes to China's South-to-North Water Diversion Project. Water Res. 2024;261:122001. https://doi.org/10.1016/j.watres.2024.122001.
17. Liang J, Yan M, Zhu Z, Lu L, Ding J, Zhou Q, et al. The role of microorganisms in phosphorus cycling at river-lake confluences: insights from a study on microbial community dynamics. Water Res. 2025;268:122556. https://doi.org/10.1016/j.watres.2024.122556.
18. Tang M, Chen Q, Xiao X, Lyu Y, Sun W. Differential impacts of water diversion and environmental factors on bacterial, archaeal, and fungal communities in the eastern route of the South-to-North water diversion project. Environ Int. 2025;195:109280. https://doi.org/10.1016/j.envint.2025.109280.
19. Rieder J, Kapopoulou A, Bank C, Adrian-Kalchhauser I. Metagenomics and metabarcoding experimental choices and their impact on microbial community characterization in freshwater recirculating aquaculture systems. Environ Microbiol. 2023;18(1):8. https://doi.org/10.1186/s40793-023-00459-z.
20. Martiny JBH, Martiny AC, Brodie E, Chase AB, Rodriguez-Verdugo A, Treseder KK, et al. Investigating the eco-evolutionary response of microbiomes to environmental change. Ecol Lett. 2023;26(S1):S81–90. https://doi.org/10.1111/ele.14209.
21. Tang X, Xie G, Shao K, Hu Y, Cai J, Bai C, et al. Contrast diversity patterns and processes of microbial community assembly in a river-lake continuum across a catchment scale in northwestern China. Environ Microbiol. 2020;15(1):10. https://doi.org/10.1186/s40793-020-00356-9.
22. Bhatnagar S, Cowley ES, Kopf SH, Perez Castro S, Kearney S, Dawson SC, et al. Microbial community dynamics and coexistence in a sulfide-driven phototrophic bloom. Environ Microbiol. 2020;15(1):3. https://doi.org/10.1186/s40793-019-0348-0.
23. Almog G, Rubin-Blum M, Murrell C, Vigderovich H, Eckert W, Larke-Mejía N, et al. Survival strategies of aerobic methanotrophs under hypoxia in methanogenic lake sediments. Environ Microbiol. 2024;19:44. https://doi.org/10.1186/s40793-024-00586-1.
24. Paquette AJ, Bhatnagar S, Vadlamani A, Gillis T, Khot V, Novotnik B, et al. Ecology and biogeochemistry of the microbial underworld in two sister soda lakes. Environ Microbiol. 2024;19(1):98. https://doi.org/10.1186/s40793-024-00632-y.
25. Liu Y, Mohamad O, Gao L, Xie Y, Abdugheni R, Huang Y, et al. Sediment prokaryotic microbial community and potential biogeochemical cycle from saline lakes shaped by habitat. Microbiol Res. 2023;270:127342. https://doi.org/10.1016/j.micres.2023.127342.
26. Sierra MA, Ryon KA, Tierney BT, Foox J, Bhattacharya C, Afshin E, et al. Microbiome and metagenomic analysis of Lake Hillier Australia reveals pigment-rich polyextremophiles and wide-ranging metabolic adaptations. Environ Microbiome. 2022;17(1):60. https://doi.org/10.1186/s40793-022-00455-9.
27. Ren Z, Qu X, Peng W, Yu Y, Zhang M. Functional properties of bacterial communities in water and sediment of the eutrophic river-lake system of Poyang Lake, China. PeerJ. 2019;7:e7318. https://doi.org/10.7717/peerj.7318.
28. Yuan X, Wang M, Guo X, Wu D. Analysis of the seasonal changes in planktonic microbial diversity in urban river supplied with reclaimed water: a case study of the North Canal River. Environ Sci. 2022;43:4097–107. https://doi.org/10.13227/j.hjkx.202112023.
29. Chen Y, Li D, Liu S, Song X, Li Z, Sun J, et al. Deposited dead algae influence the microbial communities and functional potentials on the surface sediment in eutrophic shallow lakes. Environ Res. 2025;271:121072. https://doi.org/10.1016/j.envres.2025.121072.
30. Bi Z, Wang X, Fu H, Huang Y. Carbon source shaped microbial ecology, metabolism and performance in biofilm system for simultaneous phosphorus recovery and nitrogen removal. Environ Res. 2025;286:122800. https://doi.org/10.1016/j.envres.2025.122800.
31. Ding J, Yang W, Liu X, Zhao J, Fu X, Zhang F, et al. Hydraulic conditions control the abundance of antibiotic resistance genes and their potential host microorganisms in a frequently regulated river-lake system. Sci Total Environ. 2024;946:174143. https://doi.org/10.1016/j.scitotenv.2024.174143.
32. Zhang S, Li X, Ren Z, Zhang C, Fang L, Mo X, et al. Influence of precipitation and temperature variability on anthropogenic nutrient inputs in a river watershed: implications for environmental management. J Environ Manage. 2025;375:124294. https://doi.org/10.1016/j.jenvman.2025.124294.
33. Song H, Li Z, Du B, Wang G, Ding Y. Bacterial communities in sediments of the shallow Lake Dongping in China. J Appl Microbiol. 2012;112:79–89. https://doi.org/10.1111/j.1365-2672.2011.05187.x.
34. Sun R, Wei J, Zhang S, Pei H. The dynamic changes in phytoplankton and environmental factors within Dongping Lake (China) before and after the South-to-North Water Diversion Project. Environ Res. 2024;246:118138. https://doi.org/10.1016/j.envres.2024.118138.
35. Zhao Z, Gong X, Ding Q, Jin M, Wang Z, Lu S, et al. Environmental implications from the priority pollutants screening in impoundment reservoir along the eastern route of China's South-to-North Water Diversion Project. Sci Total Environ. 2021;794:148700. https://doi.org/10.1016/j.scitotenv.2021.148700.
36. Zhou X, Lennon JT, Lu X, Ruan A. Anthropogenic activities mediate stratification and stability of microbial communities in freshwater sediments. Microbiome. 2023;11:191. https://doi.org/10.1186/s40168-023-01612-z.
37. Zhou J, Ning D. Stochastic community assembly: does it matter in microbial ecology? Microbiol Mol Biol Rev. 2017;81(4):e00002-17. https://doi.org/10.1128/MMBR.00002-17.
38. Ren Y, Yu G, Shi C, Liu L, Guo Q, Han C, et al. Majorbio Cloud: a one-stop, comprehensive bioinformatic platform for multiomics analyses. Imeta. 2022;1(2):e12. https://doi.org/10.1002/imt2.12.

39. Xun W, Liu Y, Li W, Ren Y, Xiong W, Xu Z, et al. Specialized metabolic functions of keystone taxa sustain soil microbiome stability. Microbiome. 2021;9:35. https://doi.org/10.1186/s40168-020-00985-9.
40. Hastie T, Tibshirani R. Generalized additive models: some applications. J Am Stat Assoc. 1987;82:371–86. https://doi.org/10.2307/2289439.
41. Feng X, Qin S, Zhang D, Chen P, Hu J, Wang G, et al. Nitrogen input enhances microbial carbon use efficiency by altering plant-microbe-mineral interactions. Glob Change Biol. 2022;28:4845–60. https://doi.org/10.1111/gcb.16229.
42. Gleich SJ, Cram JA, Weissman JL, Caron DA. NetGAM: using generalized additive models to improve the predictive power of ecological network analyses constructed using time-series data. ISME Commun. 2022;2(1):23. https://doi.org/10.1038/s43705-022-00106-7.
43. Blake C, Barber JN, Connallon T, McDonald MJ. Evolutionary shift of a tipping point can precipitate, or forestall, collapse in a microbial community. Nat Ecol Evol. 2024;8:2325–35. https://doi.org/10.1038/s41559-024-02543-0.
44. Shang J, Li Y, Zhang W, Ma X, Niu L, Wang L, et al. Hysteretic and asynchronous regime shifts of bacterial and micro-eukaryotic communities driven by nutrient loading. Water Res. 2024;261:122045. https://doi.org/10.1016/j.watres.2024.122045.
45. Toms J, Lesperance M. Piecewise regression: a tool for identifying ecological thresholds. Ecology. 2003;84:2034–41. https://doi.org/10.1890/02-0472.
46. Li Q, Yue Y, Wang L, Wang K. Regional differences in carbon-water dynamics of various plantation forests in Southwest China. J Hydrol. 2025;661:133809. https://doi.org/10.1016/j.jhydrol.2025.133809.
47. Li Y, Liang X, Yang N, Lin L, Gao T. Moisture-driven microbial regime shifts mediate nutrient dynamics in reservoir riparian zones. Water Res. 2025;287:124309. https://doi.org/10.1016/j.watres.2025.124309.
48. Ma R, Tian Z, Zhao Y, Wu Y, Liang Y. Response of soil quality degradation to cultivation and soil erosion: a case study in a Mollisol region of Northeast China. Soil Tillage Res. 2024;242:106159. https://doi.org/10.1016/j.still.2024.106159.
49. Deng Y, Jiang Y, Yang Y, He Z, Luo F, Zhou J. Molecular ecological network analyses. BMC Bioinf. 2012;13(1):113. https://doi.org/10.1186/1471-2105-13-113.
50. Xiao N, Zhou A, Kempher M, Zhou B, Shi Z, Yuan M, et al. Disentangling direct from indirect relationships in association networks. Proc Natl Acad Sci U S A. 2022;119:e2109995119. https://doi.org/10.1073/pnas.2109995119.
51. Peng X, Wang S, Wang M, Feng K, He Q, Yang X, et al. Metabolic interdependencies in thermophilic communities are revealed using co-occurrence and complementarity networks. Nat Commun. 2024;15:8166. https://doi.org/10.1038/s41467-024-52532-x.
52. Liu X, Nie Y, Wu X. Predicting microbial community compositions in wastewater treatment plants using artificial neural networks. Microbiome. 2023;11:93. https://doi.org/10.1186/s40168-023-01519-9.
53. Shi L, Deng Q, Lu C, Liu W. Prediction of PM_{10} mass concentrations based on BP artificial neural network. J Cent South Univ (Sci Technol). 2012;43:1969–74.
54. Li Q, Yue T, Wang C, Zhang W, Yu Y, Li B, et al. Spatially distributed modeling of soil organic matter across China: an application of artificial neural network approach. CATENA. 2013;104:210–8. https://doi.org/10.1016/j.catena.2012.11.012.
55. Tang J, Zeng X, Gao W. A high impedance-grounding fault detection method for distribution network based on empirical mode decomposition and local maximum point number. Electr Eng. 2024;25:14–23. https://doi.org/10.3969/j.issn.1673-3800.2024.06.002.
56. Li M, Yang X, Wang K, Di C, Xiang W, Zhang J. Exploring China's water scarcity incorporating surface water quality and multiple existing solutions. Environ Res. 2024;246:118191. https://doi.org/10.1016/j.envres.2024.118191.
57. Sun M, Li M, Zhou Y, Liu J, Shi W, Wu X, et al. Nitrogen deposition enhances the deterministic process of the prokaryotic community and increases the complexity of the microbial co-network in coastal wetlands. Sci Total Environ. 2023;856:158939. https://doi.org/10.1016/j.scitotenv.2022.158939.
58. Vellend M. Conceptual synthesis in community ecology. Q Rev Biol. 2010;85(2):183–206. https://doi.org/10.1086/652373.
59. Dini-Andreote F, Stegen JC, van Elsas JD, Salles JF. Disentangling mechanisms that mediate the balance between stochastic and deterministic processes in microbial succession. Proc Natl Acad Sci USA. 2015;112(11):E1326–32. https://doi.org/10.1073/pnas.1414261112.
60. Chen L, Qin X, Wang G, Teng M, Zheng Y, Yang F, et al. Oxygen influences spatial heterogeneity and microbial succession dynamics during *Baijiu* stacking process. Bioresour Technol. 2024;403:130854. https://doi.org/10.1016/j.biortech.2024.130854.
61. Guseva K, Darcy S, Simon E, Alteio LV, Montesinos-Navarro A, Kaiser C. From diversity to complexity: microbial networks in soils. Soil Biol Biochem. 2022;169:108604. https://doi.org/10.1016/j.soilbio.2022.108604.
62. Guo B, Zhang L, Sun H, Gao M, Yu N, Zhang Q, et al. Microbial co-occurrence network topological properties link with reactor parameters and reveal importance of low-abundance genera. NPJ Biofilms Microbiomes. 2022;8:3. https://doi.org/10.1038/s41522-021-00263-y.
63. Wang W, Ma C, Liu H, Fan Y, Liu G, Zhang K. Effects of hydraulic loading rate on the removal of pollutants from an integrated biological settling tank. Environ Sci. 2016;37:4727–33. https://doi.org/10.13227/j.hjkx.201605214.
64. Rong X, Zhou X, Li X, Yao M, Lu Y, Xu P, et al. Biocrust diazotrophs and bacteria rather than fungi are sensitive to chronic low N deposition. Environ Microbiol. 2022;24(11):5450–66. https://doi.org/10.1111/1462-2920.16095.
65. Fang W, Tian W, Yan D, Li Y, Cao A, Wang Q. Linkages between soil nutrient turnover and above-ground crop nutrient metabolism: the role of soil microbes. iMetaOmics. 2025;2:e55. https://doi.org/10.1002/imo2.55.
66. Jia Y, Hu X, Kang W, Dong X. Unveiling microbial nitrogen metabolism in rivers using a machine learning approach. Environ Sci Technol. 2024;58:6605–15. https://doi.org/10.1021/acs.est.3c09653.
67. Liu Y, Wei H, Dai J, Liu S, Qiu D. Microbial nitrogen removal and the molecular mechanisms underlying modulation and switching of dissimilatory nitrate reduction pathways in *Shewanella* strains. Acta Microbiol Sin. 2024;64:4656–68. https://doi.org/10.13343/j.cnki.wsxb.20240716.
68. Abdelhamed H, Nho SW, Karsi A, Lawrence ML. The role of denitrification genes in anaerobic growth and virulence of *Flavobacterium columnare*. J Appl Microbiol. 2021;130:1062–74. https://doi.org/10.1111/jam.14855.
69. Chen H, Qi L, Chen J, Xia Z, Li Q, Ao Z, et al. Mechanisms and differences of N_2O emission characteristics in typical wastewater treatment processes. Environ Sci. 2025;45:718–26. https://doi.org/10.19674/j.cnki.issn1000-6923.2025.0030.
70. Liao H, Song C, Wan L, Shi S, Wang X. Effect of chelated iron on nitrogen removal efficiency and microbial community structure in the anaerobic ferric ammonium oxidation. Environ Sci. 2021;42:4366–73. https://doi.org/10.13227/j.hjkx.202012216.
71. Huang S, Yu D, Chen G, Wang Y, Tang P, Liu C, et al. Realization of nitrite accumulation in a sulfide-driven autotrophic denitrification process: simultaneous nitrate and sulfur removal. Chemosphere. 2021;278:130413. https://doi.org/10.1016/j.chemosphere.2021.130413.
72. Cheng W, Yin Y, Li Y, Li B, Liu D, Ye L, et al. Nitrogen removal by a strengthened comprehensive floating bed with embedded pellets made by a newly isolated *Pseudomonas* sp. Y1. Environ Technol. 2024;45:208–20. https://doi.org/10.1080/09593330.2022.2102940.
73. Yang Y, Gerrity S, Collins G, Chen T, Li R, Xie S, et al. Enrichment and characterization of autotrophic *Thiobacillus* denitrifiers from anaerobic sludge for nitrate removal. Process Biochem. 2018;68:165–70. https://doi.org/10.1016/j.procbio.2018.02.017.
74. Fenn S, Dubern JF, Cigana C, De Simone M, Lazenby J, Juhas M, et al. NirA is an alternative nitrite reductase from *Pseudomonas aeruginosa* with potential as an antivirulence target. MBio. 2021;12(2):e00207. https://doi.org/10.1128/mBio.00207-21.
75. Luo Y, Luo L, Huang X, Jiang D, Wu X, Li Z. Characterization and metabolic pathway of *Pseudomonas fluorescens* 2P24 for highly efficient ammonium and nitrate removal. Bioresour Technol. 2023;382:129189. https://doi.org/10.1016/j.biortech.2023.129189.
76. Shen C, Liu S, Su J, Tian P, Dai J. Rhizosphere bacterial community structure and function of *Caragana korshinskii* in semiarid desert area. Genomics Appl Biol. 2021;40:3508–17. https://doi.org/10.13417/j.gab.040.003508.
77. Wang Z, Wang S, Liu Y, Feng K, Deng Y. The applications of metagenomics in the detection of environmental microbes involving in nitrogen cycle. Biotechnol Bull. 2018;34:1–14. https://doi.org/10.13560/j.cnki.biotech.bull.1985.2018-0024.
78. Yang Y, Pan J, Zhou Z, Wu J, Liu Y, Lin J, et al. Complex microbial nitrogen-cycling networks in three distinct anammox-inoculated wastewater treatment systems. Water Res. 2020;168:115142. https://doi.org/10.1016/j.watres.2019.115142.

Publisher's Note